Supplementary Tables and Figures

Parameter	Symbol	Value	Units	Non-dimensional
Non-dimensional parameters				
Reference Rayleigh number	Ra_S			3.0×10^{8}
Surface dissipation number	Di_S			1.2
Total internal heating	H_{tot}	21.6	mW m^{-2}	13.454
Compositional heating ratio	R_H	1-100		
Compositional parameters				
Buoyancy ratio	B_z	142	kg m^{-3}	0.23
Volume fraction of dense material (%)	X_{prim}			4.0
Physical & thermo-dynamical parameters				
Acceleration of gravity	g	9.81	m s^{-2}	1.0
Mantle thickness	D	2891	km	1.0
Reference adiabat	T_{as}	1600	K	0.64
Super-adiabatic temperature difference	ΔT_S	2500	K	1.0
Surface density	ρ_S	3300	kg m^{-3}	1.0
Surface thermal expansion	α_S	5.0×10^{-5}	K^{-1}	1.0
Surface thermal diffusivity	κ_S	7.5×10^{-7}	m^2 s^{-1}	1.0
Heat capacity	C_P	1200	J kg^{-1} K^{-1}	1.0
Surface thermal conductivity	k_S	3.0	W m^{-1} K^{-1}	1.0
Surface Grüneisen parameter	γ_S	1.091		
Density jump at z = 660 km	$\Delta\rho_{660}$	400	kg m^{-3}	0.1212
Clapeyron slope at z = 660 km	Γ_{660}	-2.5	MPa K^{-1}	-0.0668
CMB temperature	T_{CMB}	3750	K	1.5
Density jump at CMB	$\Delta\rho_{CMB}$	5280	kg m^{-3}	1.6
Viscosity law				
Reference viscosity	η_0	1.6×10^{21}	Pa s	1.0
Viscosity ratio at z = 660 km	$\Delta\eta_{660}$	30		
Logarithmic thermal viscosity ratio	E_a	16.118		
Logarithmic vertical viscosity ratio	V_a	2.303		
Compositional viscosity ratio	$\Delta\eta_C$	32		
Surface yield stress	σ_0	290	MPa	7.5×10^{6}
Yield stress gradient	$\dot{\sigma}_z$	0.01	Pa/Pa	0.01

Supplementary Table 1. Parameters and scalings of numerical simulations

a	R_H	$<T>$ (K)	dT_{neg} (K)	dT_{pos} (K)	k_{200km} ($Wm^{-1}K^{-1}$)	$<T_{slab}>$ (K)	V_{slab}	$<T_{piles}>$ (K)	k_{piles} ($Wm^{-1}K^{-1}$)	h_{piles} (km)
0.00	1	2055.2	519.3	285.0	23.93	2537.6	0.137	3354.5	21.01	553.9
0.00	10	1955.0	458.7	347.8	24.34	2577.4	0.135	3386.6	20.82	704.2
0.00	15	1926.0	388.4	308.4	23.86	2700.9	0.134	3371.1	20.93	704.8
0.00	30	1859.3	502.3	384.4	24.38	2498.2	0.150	3378.9	20.73	785.5
0.00	50	1799.1	478.9	289.5	23.62	2518.3	0.114	3334.9	21.07	616.8
0.10	1	2038.2	501.5	298.4	18.86	2547.9	0.146	3335.7	16.52	568.8
0.10	10	1921.3	581.7	387.5	19.13	2405.8	0.148	3409.6	16.39	640.4
0.10	15	1885.4	592.2	411.6	19.05	2423.7	0.181	3429.8	16.39	656.5
0.10	20	1897.4	563.0	357.9	18.95	2466.9	0.151	3393.4	16.45	608.5
0.10	30	1806.0	520.8	364.9	18.93	2493.2	0.153	3390.4	16.43	675.0
0.10	50	1765.0	521.0	355.7	18.82	2403.1	0.125	3345.8	16.47	728.1
0.15	10	1925.3	538.0	409.5	17.04	2447.3	0.160	3409.9	14.47	693.3
0.15	15	1906.7	561.3	364.7	16.90	2481.9	0.166	3400.2	14.54	651.9
0.15	20	1813.8	564.6	428.8	17.06	2453.9	0.185	3436.8	14.45	702.2
0.15	30	1802.5	546.1	399.6	16.96	2482.3	0.187	3365.9	14.53	698.6
0.15	40	1793.0	583.4	403.1	16.99	2390.6	0.161	3371.7	14.53	677.6
0.15	50	1749.5	511.6	380.9	16.80	2474.4	0.170	3320.2	14.62	685.7
0.20	1	2078.2	534.7	326.6	15.06	2435.0	0.140	3315.8	12.94	630.7
0.20	5	1932.7	486.7	308.8	14.72	2568.3	0.144	3359.5	13.00	571.8
0.20	10	1931.8	580.3	403.9	15.06	2413.9	0.161	3415.8	12.86	629.5
0.20	15	1852.5	553.4	422.7	15.14	2382.4	0.146	3407.5	12.82	729.7
0.20	20	1853.4	639.8	435.7	15.13	2381.5	0.192	3439.0	12.84	632.4
0.20	30	1821.5	646.8	454.0	15.20	2350.1	0.195	3424.8	12.82	629.1
0.20	40	1789.1	571.1	423.9	15.13	2395.8	0.179	3365.6	12.87	701.6
0.20	50	1777.4	556.4	355.4	14.85	2450.6	0.167	3349.9	12.97	637.8
0.30	1	2025.1	446.2	278.3	11.58	2512.3	0.112	3317.1	10.26	578.2
0.30	5	1956.3	631.7	396.3	11.91	2391.6	0.189	3396.2	10.12	572.9
0.30	10	1926.2	656.0	440.2	11.97	2297.5	0.166	3447.4	10.06	602.4
0.30	15	1874.0	616.9	481.3	12.07	2333.1	0.171	3470.4	10.00	663.1
0.30	20	1804.0	588.5	437.5	11.87	2326.8	0.143	3441.1	10.08	672.0
0.30	30	1735.2	569.3	426.1	11.89	2375.4	0.165	3379.1	10.13	687.8
0.30	40	1772.2	664.6	497.4	12.11	2302.4	0.205	3433.5	10.04	638.2
0.30	50	1759.0	631.1	502.0	12.19	2318.5	0.207	3417.7	10.00	727.4
0.30	80	1752.4	557.8	512.3	12.36	2279.6	0.161	3365.2	9.96	774.7
0.30	100	1713.0	581.0	452.2	12.17	2291.4	0.160	3296.8	10.13	685.8

Supplementary Table 2. Thermal and compositional output parameters averaged out over the last 2 Gyr of the simulations. Listed parameters are the average temperature, $<T>$, *rms* positive and negative temperature anomalies in the bottom 200 km, dT_{neg} and dT_{pos}, average thermal conductivity in the bottom 200 km, k_{200km}, slabs average temperature and volume fraction in the bottom 200 km, $<T_{slab}>$ and V_{slab}, and the thermo-chemical piles average temperature, $<T_{piles}>$, thermal conductivity, k_{piles}, and maximum altitude, h_{piles}.

a	R_H	$<T>$ (K)	dT_{neg} (K)	dT_{pos} (K)	k_{200km} ($Wm^{-1}K^{-1}$)	$<T_{slab}>$ (K)	V_{slab}	$<T_{piles}>$ (K)	k_{piles} ($Wm^{-1}K^{-1}$)	h_{piles} (km)
0.35	3	2034.2	614.9	413.0	10.68	2367.5	0.189	3384.5	8.94	669.2
0.35	4	1986.4	590.2	408.9	10.62	2360.3	0.164	3403.4	8.94	652.9
0.35	5	1999.1	586.7	401.8	10.62	2387.0	0.159	3404.8	8.93	650.1
0.35	10	1927.7	688.2	453.3	10.64	2269.6	0.181	3449.9	8.92	618.3
0.40	1	2051.9	613.5	325.6	9.33	2401.0	0.164	3314.5	8.05	589.6
0.40	3	2031.7	652.8	381.4	9.41	2313.4	0.159	3372.0	7.98	591.0
0.40	4	2011.4	657.5	384.8	9.38	2338.4	0.174	3391.3	7.97	585.7
0.40	5	1990.6	638.3	394.9	9.39	2354.3	0.170	3410.5	7.94	618.1
0.40	10	1936.7	628.5	492.8	9.56	2270.1	0.160	3504.2	7.78	768.4
0.40	15	1868.3	606.7	554.7	9.68	2263.5	0.160	3498.7	7.77	725.6
0.40	20	1838.1	645.5	496.6	9.54	2284.8	0.176	3481.0	7.82	717.8
0.40	30	1795.9	603.9	506.1	9.59	2317.6	0.170	3462.1	7.81	711.5
0.40	50	1735.5	700.9	547.3	9.72	2207.5	0.214	3448.7	7.83	686.9
0.50	1	2094.9	631.3	334.6	7.40	2363.5	0.176	3319.4	6.33	559.1
0.50	2	2018.9	615.0	308.1	7.23	2334.0	0.131	3356.6	6.33	545.6
0.50	3	2020.4	669.9	371.8	7.40	2337.3	0.182	3372.5	6.28	555.6
0.50	4	2020.6	640.1	386.9	7.38	2335.8	0.160	3408.2	6.24	626.8
0.50	5	1990.8	710.6	459.0	7.52	2299.8	0.215	3459.6	6.17	647.4
0.50	10	1943.1	711.0	520.6	7.57	2242.9	0.190	3534.6	6.09	687.2
0.50	15	1866.1	684.2	566.6	7.63	2281.5	0.216	3550.4	6.06	702.3
0.50	20	1823.3	778.9	564.2	7.62	2223.0	0.236	3549.7	6.08	647.4
0.50	30	1734.9	637.1	579.5	7.66	2266.8	0.203	3516.8	6.07	816.8
0.50	50	1709.4	656.1	607.2	7.77	2207.7	0.201	3498.7	6.07	791.2
0.50	100	1684.0	650.4	499.0	7.66	2265.2	0.221	3348.8	6.26	680.8
0.60	1	2068.8	581.1	362.0	5.90	2356.7	0.168	3333.1	4.96	597.3
0.60	2	2051.1	659.5	407.0	5.96	2248.5	0.157	3381.1	4.90	628.6
0.60	3	2032.8	614.4	358.3	5.79	2356.4	0.148	3384.0	4.93	577.4
0.60	4	2031.7	720.4	464.8	5.98	2229.0	0.177	3453.0	4.84	632.8
0.60	5	2006.4	734.9	471.0	5.95	2233.8	0.188	3474.4	4.83	572.7
0.60	10	1912.9	726.7	592.9	6.09	2202.1	0.207	3584.4	4.71	705.2
0.60	15	1885.9	771.0	608.3	6.06	2186.3	0.213	3613.6	4.70	650.6
0.60	20	1829.3	775.2	627.7	6.12	2125.4	0.201	3600.6	4.70	683.1
0.60	30	1777.7	739.4	545.3	5.92	2242.9	0.205	3550.1	4.78	678.2
0.60	50	1741.6	736.4	609.7	6.14	2180.2	0.222	3540.4	4.74	669.2

Supplementary Table 2, continued.

a	R_H	$<T>$ (K)	dT_{neg} (K)	dT_{pos} (K)	k_{200km} ($Wm^{-1}K^{-1}$)	$<T_{slab}>$ (K)	V_{slab}	$<T_{piles}>$ (K)	k_{piles} ($Wm^{-1}K^{-1}$)	h_{piles} (km)
0.80	1	2109.7	688.3	335.3	3.67	2261.0	0.155	3326.6	3.09	508.5
0.80	2	2080.0	670.1	394.7	3.69	2320.8	0.179	3409.0	3.01	601.2
0.80	3	2095.2	683.8	598.3	3.87	2242.3	0.218	3591.6	2.86	664.6
0.80	5	2049.5	778.8	608.5	3.83	2211.1	0.210	3668.6	2.83	690.2
0.80	10	1955.3	831.3	710.7	3.87	2179.5	0.256	3825.9	2.73	840.0
0.80	15	1906.4	830.1	747.2	3.84	2218.3	0.256	3859.1	2.71	735.5
0.80	20	1829.7	905.8	687.4	3.83	2179.7	0.263	3742.7	2.79	646.1
0.80	30	1786.8	859.5	735.2	3.94	2131.3	0.275	3774.7	2.76	877.0
0.80	50	1753.2	831.2	743.7	3.95	2094.1	0.238	3720.9	2.79	731.0
1.00	1	2158.9	748.6	344.1	2.31	2176.9	0.130	3351.4	1.90	481.4
1.00	2	2153.8	750.7	593.2	2.44	2199.4	0.196	3632.3	1.73	643.9
1.00	10	2032.4	761.7	874.1	2.57	2153.5	0.241	4122.7	1.52	1386.0
1.00	15	1956.0	815.6	793.4	2.51	2144.4	0.254	4004.9	1.57	1480.3
1.00	20	1913.7	764.5	956.9	2.68	2115.0	0.291	4082.6	1.50	1654.8
1.00	30	1885.8	788.2	897.0	2.69	2010.6	0.249	3826.9	1.66	1209.9
1.00	50	1820.4	672.5	1037.0	2.81	1949.8	0.204	4053.9	1.53	1284.9

Supplementary Table 2, continued.

a	R_H	$\langle\Phi\rangle$ (mW m^{-2})	Φ_{min} (mW m^{-2})	Φ_{max} (mW m^{-2})	$\delta\Phi$	S_{neg}	$\langle\Phi_{neg}\rangle$ (mW m^{-2})	P_{neg} (TW)	S_{sub}	$\langle\Phi_{sub}\rangle$ (mW m^{-2})
0.00	1	139.4	24.5	514.1	1.76	-	-	-	0.549	42.1
0.00	10	137.6	10.6	461.3	1.64	-	-	-	0.491	26.4
0.00	15	121.5	8.3	387.6	1.56	-	-	-	0.455	29.6
0.00	30	150.1	4.8	509.8	1.67	-	-	-	0.459	24.5
0.00	50	131.3	18.1	489.2	1.80	-	-	-	0.487	39.7
0.10	1	113.8	19.4	407.0	1.70	-	-	-	0.566	35.4
0.10	10	122.3	6.0	456.9	1.85	-	-	-	0.540	19.7
0.10	15	127.4	3.1	453.4	1.77	-	-	-	0.534	18.8
0.10	20	115.1	5.0	425.8	1.83	-	-	-	0.563	21.3
0.10	30	112.9	3.6	406.5	1.79	-	-	-	0.522	22.5
0.10	50	115.6	7.8	443.5	1.89	-	-	-	0.512	28.7
0.15	10	110.8	0.1	394.2	1.78	-	-	-	0.522	16.6
0.15	15	104.1	0.5	378.2	1.81	-	-	-	0.571	18.7
0.15	20	111.2	-4.0	382.0	1.74	0.093	-2.5	-0.038	0.526	15.5
0.15	30	112.7	-3.2	375.7	1.68	0.053	-2.2	-0.022	0.535	22.1
0.15	40	114.8	2.8	409.2	1.77	-	-	-	0.547	21.6
0.15	50	111.2	6.3	370.8	1.64	-	-	-	0.511	26.4
0.20	1	102.4	15.7	378.4	1.77	-	-	-	0.576	28.6
0.20	5	82.6	10.5	308.7	1.81	-	-	-	0.605	26.5
0.20	10	97.9	0.5	372.3	1.90	-	-	-	0.556	15.6
0.20	15	99.6	-6.5	375.0	1.92	0.093	-4.3	-0.062	0.534	14.9
0.20	20	104.6	-1.9	380.8	1.83	0.057	-1.1	-0.011	0.566	11.7
0.20	30	109.8	-1.0	390.7	1.79	0.030	-0.7	-0.006	0.553	12.3
0.20	40	103.4	-1.6	363.3	1.76	0.034	-1. 1	-0.007	0.536	17.9
0.20	50	93.5	4.5	342.2	1.81	-	-	-	0.593	24.7
0.30	1	66.6	10.9	252.2	1.81	-	-	-	0.661	30.3
0.30	5	84.7	5.8	313.9	1.82	-	-	-	0.603	15.6
0.30	10	84.0	-2.8	339.5	2.04	0.13166	-1.5	-0.030	0.581	9.0
0.30	15	85.5	-11.6	320.6	1.94	0.21128	-5.6	-0.180	0.550	7.0
0.30	20	75.5	-7.8	314.8	2.14	0.18407	-3.9	-0.108	0.586	12.1
0.30	30	78.8	-5.8	294.3	1.91	0.14314	-3.2	-0.069	0.589	16.3
0.30	40	92.6	-3.4	324.4	1.77	0.16247	-1.8	-0.045	0.557	8.8
0.30	50	93.8	-5.6	315.1	1.71	0.12405	-3.4	-0.066	0.533	9.9
0.30	80	95.5	-2.4	320.5	1.62	0.10017	-1.5	-0.022	0.472	11.4
0.30	100	93.0	5.5	314.0	1.66	-	-	-	0.536	18.2

Supplementary Table 3. CMB heat flux parameters over the last 2 Gyr of the simulations. Listed parameters are the average, minimum and maximum heat flux CMB , $\langle\Phi\rangle$, Φ_{min} and Φ_{max}, the heat flux heterogeneity, $\delta\Phi$, the fraction of CMB area with negative heat flux, S_{neg} (dash symbol indicate that patches of negative heat flux are not observed), the average negative heat flux and total power in negative patches, $\langle\Phi_{neg}\rangle$ and P_{neg}, CMB area fraction with subadiabtic heat flux (assuming Φ_{adia}^{core} = 70 mW/m^2), S_{sub}, and the average heat flux in 'subadiabtic' regions, $\langle\Phi_{sub}\rangle$.

a	R_H	$\langle\Phi\rangle$ (mW m^{-2})	Φ_{min} (mW m^{-2})	Φ_{max} (mW m^{-2})	$\delta\Phi$	S_{neg}	$\langle\Phi_{neg}\rangle$ (mW m^{-2})	P_{neg} (TW)	S_{sub}	$\langle\Phi_{sub}\rangle$ (mW m^{-2})
0.35	3	81.9	3.8	305.3	1.84	-	-	-	0.591	15.3
0.35	4	75.8	1.2	293.3	1.93	-	-	-	0.603	16.2
0.35	5	73.6	-1.7	285.1	1.95	0.061	-1.1	-0.011	0.591	13.1
0.35	10	77.2	-5.2	315.8	2.08	0.147	-2.6	-0.060	0.597	7.5
0.40	1	68.7	11.5	268.4	1.87	-	-	-	0.665	21.2
0.40	3	70.3	4.2	291.6	2.04	-	-	-	0.634	15.2
0.40	4	68.5	1.4	276.3	2.01	-	-	-	0.638	13.7
0.40	5	66.2	-1.5	269.3	2.05	0.050	-0.9	-0.008	0.641	13.2
0.40	10	69.3	-15.9	286.1	2.19	0.223	-9.0	-0.301	0.587	8.3
0.40	15	72.3	-15.5	278.4	2.03	0.324	-7.7	-0.380	0.542	5.3
0.40	20	68.0	-17.3	271.1	2.12	0.222	-9.2	-0.306	0.588	6.9
0.40	30	66.6	-13.3	248.3	1.97	0.275	-7.2	-0.300	0.561	6.3
0.40	50	80.1	-9.3	287.3	1.85	0.249	-4.8	-0.180	0.563	7.4
0.50	1	57.6	8.1	229.2	1.92	-	-	-	0.687	18.0
0.50	2	46.8	5.9	226.1	2.36	-	-	-	0.768	19.4
0.50	3	55.3	3.1	232.6	2.07	-	-	-	0.677	13.2
0.50	4	51.9	-2.7	226.7	2.21	0.091	-1.7	-0.024	0.696	13.6
0.50	5	59.5	-6.5	238.3	2.06	0.154	-3.9	-0.092	0.644	8.5
0.50	10	57.7	-16.0	248.4	2.29	0.313	-7.4	-0.352	0.621	4.6
0.50	15	58.1	-16.1	227.5	2.10	0.395	-8.2	-0.494	0.585	1.7
0.50	20	61.4	-14.1	241.7	2.08	0.416	-7.7	-0.485	0.612	1.1
0.50	30	57.0	-21.7	215.9	2.09	0.281	-9.8	-0.418	0.611	8.7
0.50	50	62.6	-15.9	227.7	1.95	0.286	-8.0	-0.349	0.561	5.9
0.50	100	62.5	-3.4	214.0	1.74	0.112	-2.2	-0.039	0.622	14.5
0.60	1	44.9	4.2	182.3	2.00	-	-	-	0.729	17.7
0.60	2	48.2	0.4	213.2	2.20	-	-	-	0.694	13.9
0.60	3	38.5	-2.2	180.1	2.38	0.095	-14	-0.023	0.765	14.8
0.60	4	49.7	-6.0	216.1	2.24	0.146	-3.9	-0.086	0.668	9.1
0.60	5	47.5	-5.7	213.6	2.31	0.245	-3.3	-0.124	0.674	7.6
0.60	10	49.2	-15.6	207.6	2.27	0.410	-7.5	-0.465	0.623	3.9
0.60	15	47.6	-19.4	207.0	2.38	0.449	-9.4	-0.642	0.634	1.6
0.60	20	49.5	-19.3	214.2	2.37	0.424	-9.2	-0.595	0.620	1.8
0.60	30	40.7	-21. 6	189.7	2.60	0.380	-9.3	-0.537	0.704	5.6
0.60	50	49.4	-15.2	192.9	2.11	0.406	-7.5	-0.461	0.618	4.1

Supplementary Table 3, continued.

a	R_H	$\langle\Phi\rangle$ (mW m^{-2})	Φ_{min} (mW m^{-2})	Φ_{max} (mW m^{-2})	$\delta\Phi$	S_{neg}	$\langle\Phi_{neg}\rangle$ (mW m^{-2})	P_{neg} (TW)	S_{sub}	$\langle\Phi_{sub}\rangle$ (mW m^{-2})
0.80	1	29.9	2.9	145.7	2.39	-	-	-	0.823	14.1
0.80	2	28.5	-2.1	133.8	2.38	0.146	-1.4	-0.032	0.826	13.8
0.80	3	35.4	-8.2	147.3	2.21	0.318	-5.2	-0.250	0.735	12.6
0.80	5	33.3	-13.3	154.1	2.52	0.393	-6.7	-0.399	0.742	8.5
0.80	10	33.4	-23.1	151.6	2.62	0.468	-10.0	-0.714	0.714	5.2
0.80	15	30.5	-24.6	139.1	2.70	0.465	-12.2	-0.865	0.733	5.1
0.80	20	30.7	-19.6	144.7	2.70	0.509	-10.9	-0.844	0.724	2.3
0.80	30	34.7	-20.4	148.0	2.44	0.439	-10.7	-0.715	0.695	3.8
0.80	50	33.5	-20.0	144.9	2.46	0.450	-10.1	-0.691	0.732	8.2
1.00	1	20.3	0.8	117.3	2.90	-	-	-	0.904	12.8
1.00	2	23.9	-5.8	114.8	2.53	0.352	-3.8	-0.203	0.891	16.0
1.00	10	26.0	-20.1	114.1	2.62	0.378	-9.8	-0.567	0.845	14.8
1.00	15	20.5	-17.8	106.4	3.05	0.439	-9.9	-0.664	0.885	12.1
1.00	20	27.7	-17.3	103.2	2.19	0.394	-10.6	-0.638	0.847	17.5
1.00	30	27.9	-18.6	122.5	2.55	0.412	-9.3	-0.583	0.835	15.8
1.00	50	30.5	-17.3	114.8	2.17	0.322	-9.9	-0.489	0.877	22.2

Supplementary Table 3, continued.

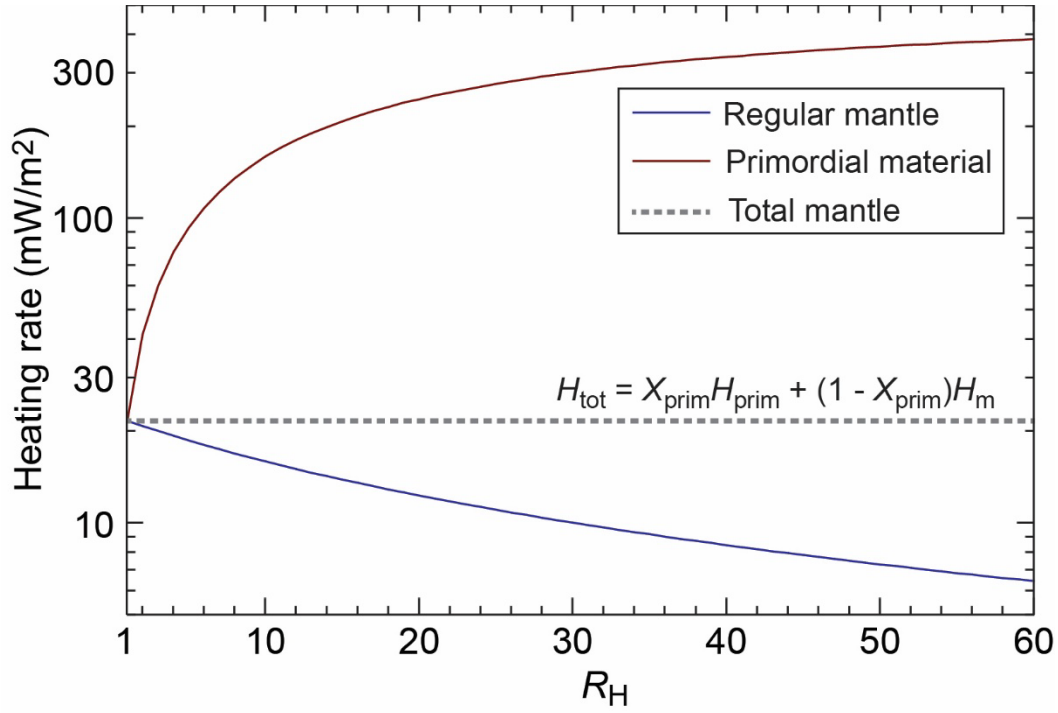

Supplementary Figure 1. Internal heating rate in the regular mantle, H_m, and in the primordial material, H_{prim}, as a function of the excess heating ratio in primordial material, R_H, and for a total heating rate H_{tot} equivalent to surface heat flux of 21.6 mW/m^2 and a volume fraction of primordial material X_{prim} equal to 4 %.

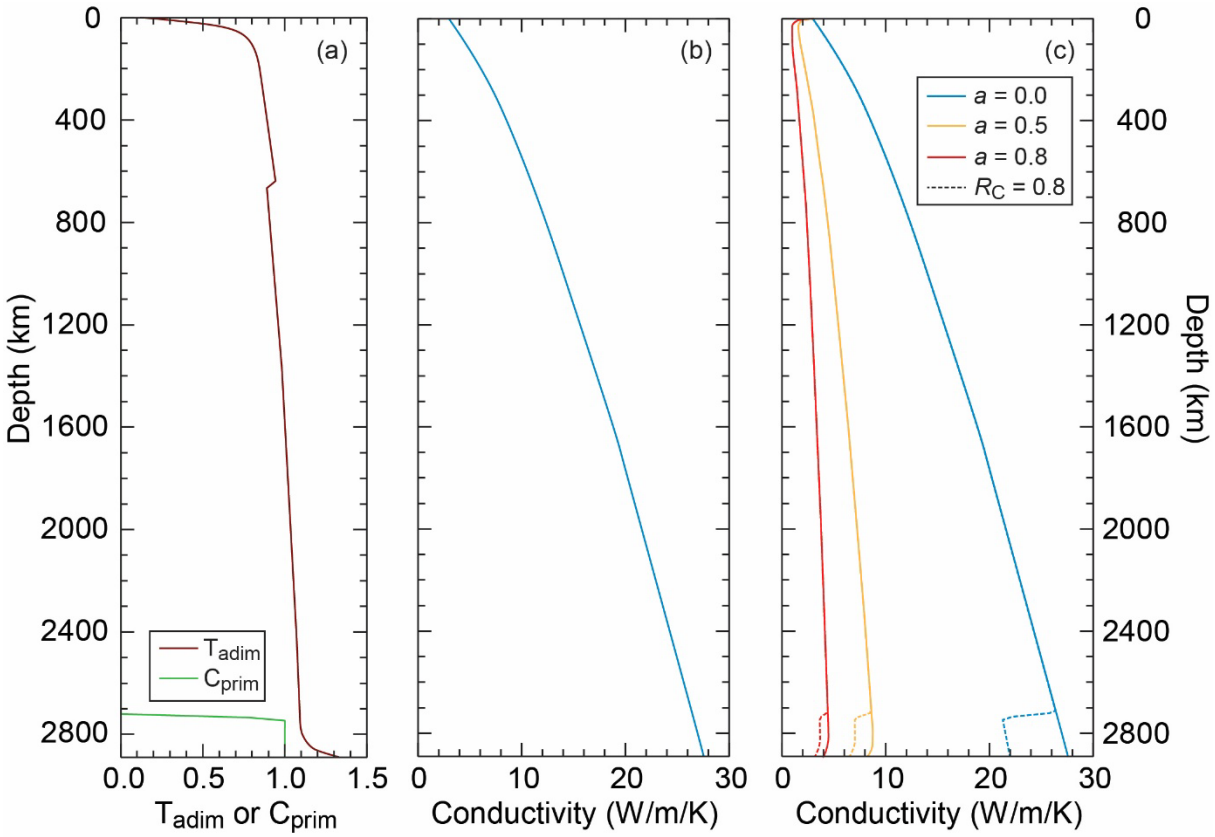

Supplementary Figure 2. Depth, temperature and compositional dependence of thermal conductivity. Panel (b) shows the intrinsic depth dependence, based on the parameterization of Deschamps and Hsieh (2019). Panel (c) shows the temperature dependence (plain lines) and the combined thermal and compositional dependences (dashed lines) corresponding to the radial models of temperature and composition plotted in panel (a) and for 3 values of the temperature exponent a and (in the case of compositional dependence) $R_C = 0.8$ (equivalent to a 20 % reduction of conductivity with composition).

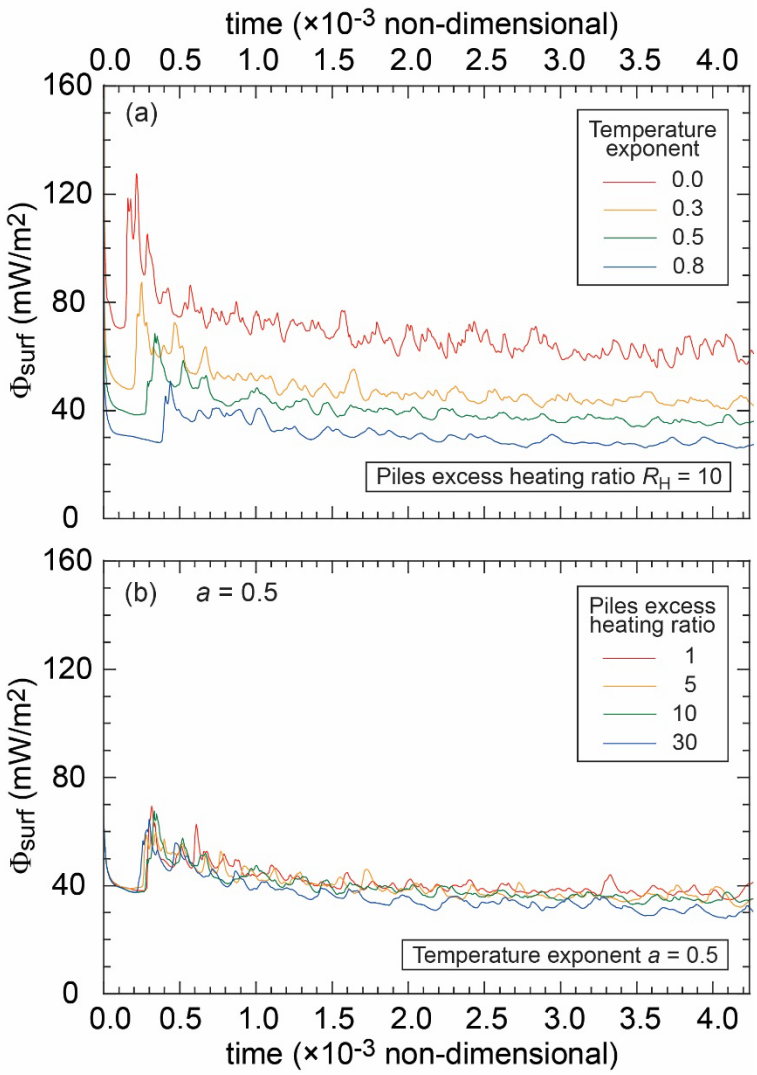

Supplementary Figure 3. Evolution of the surface heat flux for selected simulations with different temperature-dependence of thermal conductivity, controlled with the temperature exponent a, and excess heating ratio in piles of dense material, R_H. In panel (A) R_H is fixed to 10 and 4 values of a are considered (see legend). In panel (B), a is fixed to 0.5 and 4 values of R_H are considered (see legend).

Supplementary videos. Supplementary movies show the evolution show the evolution of the non-dimensional and adiabatic temperature field for 4 cases:

- Supplementary Video 1: case HR038, with $a = 0.3$ and $R_H = 15$
- Supplementary Video 2: case HR011, with $a = 0.0$ and $R_H = 1$
- Supplementary Video 3: case HR001, with $a = 0.5$ and $R_H = 10$
- Supplementary Video 4: case HR051, with $a = 0.3$ and $R_H = 30$